広島大学学術情報リポジトリ
Hiroshima University Institutional Repository

| | |
|---|---|
| Title | Structure and Thermal Transformations of Methylammonium Tungstate |
| Author(s) | Sukmana, Ndaru Candra; Sugiarto, ; Zhang, Zhenxin; Sadakane, Masahiro |
| Citation | Zeitschrift fur anorganische und allgemeine Chemie , 647 (19) : 1930 - 1937 |
| Issue Date | 2021-10-12 |
| DOI | 10.1002/zaac.202100219 |
| Self DOI | |
| URL | https://ir.lib.hiroshima-u.ac.jp/00051394 |
| Right | This is the peer reviewed version of the following article: N. Candra Sukmana Sugiarto, Z. Zhang, M. Sadakane, Z. Anorg. Allg. Chem. 2021, 647, 1930., which has been published in final form at https://doi.org/10.1002/zaac.202100219. This article may be used for non-commercial purposes in accordance with Wiley Terms and Conditions for Use of Self-Archived Versions. This article may not be enhanced, enriched or otherwise transformed into a derivative work, without express permission from Wiley or by statutory rights under applicable legislation. Copyright notices must not be removed, obscured or modified. The article must be linked to Wiley's version of record on Wiley Online Library and any embedding, framing or otherwise making available the article or pages thereof by third parties from platforms, services and websites other than Wiley Online Library must be prohibited.<br>This is not the published version. Please cite only the published version. この論文は出版社版ではありません。引用の際には出版社版をご確認、ご利用ください。 |

| Relation | |
|---|---|

# Structure and Thermal Transformations of Methylammonium Tungstate

Ndaru Candra Sukmana,[a] Sugiarto,[a] Zhenxin Zhang,[b] and Masahiro Sadakane*[a]

**Abstract:** Methylammonium paradodecatungstate, $(CH_3NH_3)_{10}[H_2W_{12}O_{42}]\cdot nH_2O$, was prepared by the reaction of $WO_3$ or $H_2WO_4$ in aqueous methylamine, followed by drying. The $[H_2W_{12}O_{42}]^{10-}$ anion consists of two $HW_3O_{13}$ groups containing three edge-sharing $WO_6$ octahedra and two $W_3O_{14}$ groups having two edge-sharing connections. On drying the produced material at 70 °C, some lattice water was released, but this did not affect the $[H_2W_{12}O_{42}]^{10-}$ structure, although there was a decrease in the unit cell volume. By adding water, the loss of lattice water and structural changes were reversed. The existence of paradodecatungstate anions was confirmed by single-crystal and powder X-ray diffraction, Fourier transform infrared, Raman, $^{183}W$ nuclear magnetic resonance, and ultraviolet–visible spectroscopy. When the methylammonium paradodecatungstate was heated to more than 150 °C, $CH_3NH_2$ and $H_2O$ were released, and amorphous $WO_3$ was observed as an intermediate product and monoclinic $WO_3$ as the final product. These results reveal the structure of methylammonium tungstate, which was first reported in 1909 and now is used as an important negative staining reagent for virus observation, is methylammonium paradodecatungstate.

## Introduction

Polyoxometalates are discrete metal oxide anions of tungsten, molybdenum, vanadium, or niobium in their highest oxidation states.[1] Polyoxometalates are modifiable substances that show rich acid-base, redox, and photolytic properties[1–3] and have been developed for applications in electrocatalysis,[4] catalysis,[5–7] and energy storage and conversion.[8] Furthermore, polyoxometalates can act as transferable building blocks that can be used for the development of new materials because of their controllable size and shape.[9,10]

Isopolyoxotungstate is one of the most important polyoxometalates[11] and is a building block for polyoxometalate-based compounds,[1–3,10] a tungsten oxide precursor,[12–14] and a staining reagent.[15] It is also one of the tungsten species extracted from tungsten ore.[16,17] The formation of isopolyoxotungstate is dependent on the pH. Specifically, the acidification of $[WO_4]^{2-}$ in aqueous solution can produce various isopolyoxotungstates via condensation reactions, resulting in $[W_7O_{24}]^{6-}$, $[H_2W_{12}O_{42}]^{10-}$, $[H_4W_{22}O_{74}]^{12-}$, $[H_{10}W_{34}O_{116}]^{18-}$, $[H_2W_{12}O_{40}]^{6-}$, $[W_{10}O_{32}]^{4-}$, $[W_6O_{19}]^{2-}$, $[H_{12}W_{36}O_{120}]^{12-}$, and $[H_4W_{19}O_{62}]^{6-}$ (Scheme 1).[1,18–22] Isopolyoxotungstates have also been formed by dissolving $H_2WO_4$ or $WO_3$ in solutions of volatile bases such as $NH_3$, $CH_3NH_2$, $(CH_3)_2NH$, and $(CH_3)_3N$ and subsequent drying (Scheme 2).[23–27] The most widely used isopolyoxotungstate compounds are $(NH_4)_{10}H_2W_{12}O_{42}$ and $(NH_4)_6H_2W_{12}O_{40}$, so-called ammonium paratungstate and ammonium metatungstate, respectively, which are commercially available.

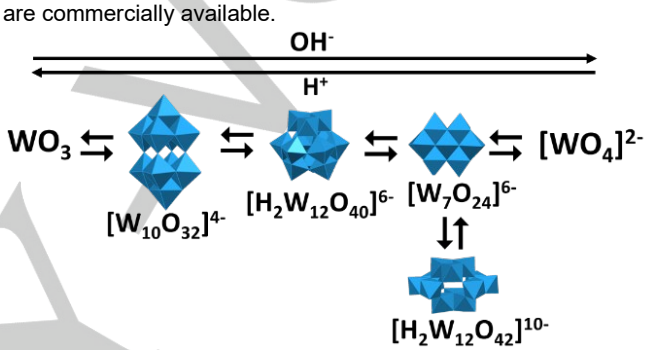


**Scheme 1.** Effect of acidity on the formation of isopolyoxotungstate. Blue polyhedra are $WO_6$ octahedra

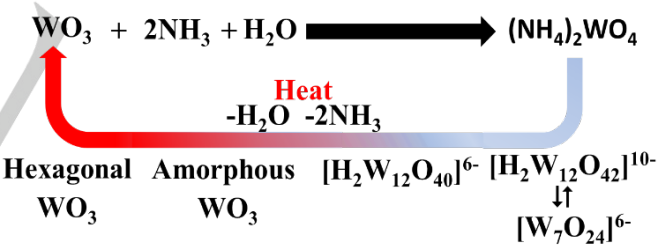


**Scheme 2.** Formation of isopolyoxotungstate by reaction of $WO_3$ and $NH_3$ and subsequent heating

In 1909, Ekeley reported that the dissolution of $H_2WO_4$ in an aqueous methylamine solution and subsequent drying at 105 °C followed by recrystallization produced methylammonium tungstate.[23] The structure of methylammonium tungstate produced by Ekeley's method was reported to be heptatungstate. Methylammonium tungstate is a successful staining reagent for the observation of bioparticles, such as viruses.[28–30]

Recently, Morajkar and Srinivasan reported that the reaction of $H_2WO_4$ and excess aqueous methylamine at room temperature, followed by slow drying at room temperature, produces single crystals of methylammonium paradodecatungstate $(CH_3NH_3)_{10}[H_2W_{12}O_{42}]\cdot 12H_2O$ in solution.[27] Intriguingly, two different structures were produced from the same reaction mixture: one produced by complete drying at 105 °C and the other produced by crystallization at room temperature.

[a] N. C. Sukmana, Dr. Sugiarto, Prof. M. Sadakane
Department of Applied Chemistry, Graduate School of Engineering
Hiroshima University
1-4-1 Kagamiyama, Higashi-Hiroshima 739-8527, Japan
E-mail: sadakane09@hiroshima-u.ac.jp
[b] Dr. Z. Zhang
School of Materials Science and Chemical Engineering,
Ningbo University
Fenghua Road 818, Ningbo, Zhejiang 315211, China

Supporting information for this article is given via a link at the end of the document.

WILEY

We are interested in identifying polyoxometalates as negative staining reagents[31,32] and are particularly interested in the structure of methylammonium tungstate. In this study, we reveal that $(CH_3NH_3)_{10}[H_2W_{12}O_{42}]\cdot nH_2O$ (methylammonium paradodecatungstate) can be synthesized from the reaction of $WO_3$ or $H_2WO_4$ with methylamine solution and subsequent drying both at room temperature and at temperatures up to 150 °C. The crystal packing of methylammonium paradodecatungstate can be reversibly changed by drying and by the re-addition of water. In addition, several tungsten-oxide-based compounds can be prepared via the thermal decomposition of paradodecatungstate.[11,33,34] The thermal transformation of methylammonium paradodecatungstate to tungsten oxide is also reported.

**Table 1.** Reaction conditions and product yield.[a)]

| Reaction temp. | $WO_3$ (g) | $H_2WO_4$ (g) | Methylamine solution (40%, mL) | Molar ratio (methylamine:W) | Solid obtained after reaction[b)] (g) | Solid obtained after evaporation of the filtrate[c)] (g) |
|---|---|---|---|---|---|---|
| Room temp. | 0.07 | - | 7 | 209 | 0.06 (solid A) | 0.02 (solid B) |
| Room temp. | - | 0.07 | 1 | 32 | - | 0.10 (solid C) |
| 70 °C | 5.22 | - | 5 | 2 | 3.14 (solid D) | 1.60 (solid E) |
| 70 °C | - | 5.63 | 5 | 2 | 1.04 (solid F) | 5.56 solid G) |

a) Reaction performed for 2 h. b) Solid obtained by filtration and subsequent drying at 70 °C. c) Solid obtained by heating to 70 °C.

## Results and Discussion

### Synthesis

Synthetic methods similar to those used by Ekeley[23] and Srinivasan[27] were used: $WO_3$ or $H_2WO_4$ was reacted with aqueous methylamine solution at room temperature or 70 °C for 2 h (Table 1). At room temperature, $WO_3$ was not completely dissolved in excess methylamine solution. Thus, the undissolved solid (solid A) was separated by filtration. The filtrate was then evaporated at 70 °C under atmospheric pressure to obtain solid B. Powder X-ray diffraction (XRD) measurements confirmed that solid A, which was not dissolved in methylamine solution at room temperature, is $WO_3$ (Figure S1, profile b). The XRD pattern of solid B obtained by the evaporation of the filtrate indicates the formation of a crystalline material (Figure S1, profile c).

In contrast, $H_2WO_4$ completely dissolved in the methylamine solution at room temperature at a methylamine/tungsten ratio of 32. The solution was evaporated at 70 °C at atmospheric pressure to form a white powder (solid C). As shown in profile d in Figure 1, the powder XRD pattern of solid C is similar to that of solid B (see also Figure S1, profile d).

As an alternative method, $WO_3$ or $H_2WO_4$ was mixed with aqueous methylamine solution in a methylamine/W ratio of 2 and stirred at room temperature for 30 min in a Teflon beaker. The mixture was heated at 70 °C for 2 h in a stainless-steel autoclave with Teflon liner (closed system) to prevent the evaporation of methylamine and water during the reaction, and the formed solids were separated by filtration to obtain solids D (wet) and F (wet), which were subsequently dried at 70 °C to form solids D and F. The filtrates were evaporated at 70 °C at atmospheric pressure to form a white solid powder (solid E and G). The XRD patterns of solids D (wet) and F (wet) (Figure 1, profiles a and b) differ from that of $WO_3$ and show peaks at low angles (< 10°, i.e., *d*-spacing larger than 8.8 Å), indicating that a new crystalline tungstate was formed. On the other hand, the XRD profiles of solids D, E, F, and G, which had been heated at 70 °C, are similar to that of solid C, indicating that the heating of solids D (wet) and F (wet) at 70 °C changed their crystal structures. Furthermore, the powder XRD pattern of solid E (wet), which was obtained before the complete drying of the filtrate at 70 °C, is similar to those of solids D (wet) and F (wet).

These results indicate that the same tungstate species were produced by dissolving $H_2WO_4$ or $WO_3$ in aqueous methylamine solution at room temperature and 70 °C, and solids D (wet) and F (wet) were precipitated by cooling the solution to room temperature. In addition, although the peak positions in the XRD patterns are the same, the peak intensity ratios are different, possibly because of preferred orientation effects; that is, preferential growth along one axis results in an anisotropic particle shape. In addition, the drying of the wet solid changed the powder XRD pattern. Next, the structural similarity of solids D and E was confirmed by FT-IR (Figure S2). In addition, the solid yield obtained after the evaporation of the filtrate synthesized from $H_2WO_4$ was higher than that from $WO_3$.

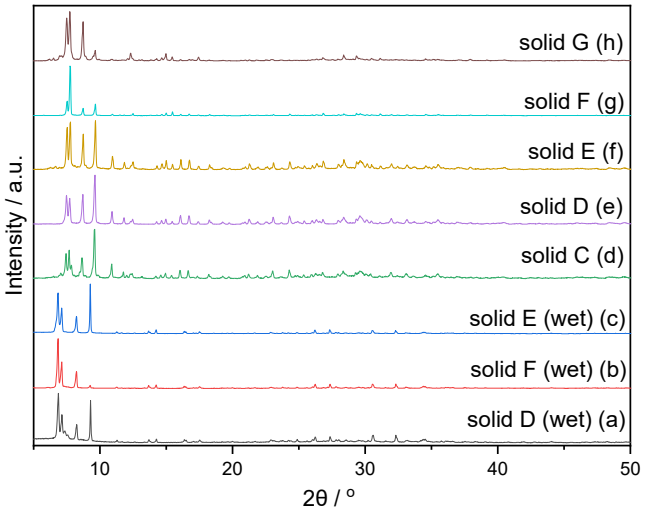

**Figure 1.** XRD patterns of solids D (wet) (a), F (wet) (b), E (wet) (c), C (d), D (e), E (f), F (g), and G (h).

### Crystal structure

Colorless single crystals suitable for X-ray structure analysis were obtained by slow ethanol diffusion into an aqueous solution of solid E. The XRD analysis revealed that $[H_2W_{12}O_{42}]^{10-}$ crystallized in the triclinic space group $P\bar{1}$ together with ten methylammonium counter-cations and twelve water molecules (Table 2), which is same to the crystal structure of $(CH_3NH_3)_{10}[H_2W_{12}O_{42}]\cdot 12H_2O$ reported by Morajkar and Srinivasan.[27] The $[H_2W_{12}O_{42}]^{10-}$ anion is structurally identical to the anions of $(NH_4)_{10}[H_2W_{12}O_{42}]\cdot 4H_2O$,[33] $(NH_4)_7[Bi(H_2W_{12}O_{42})]\cdot 20H_2O$,[35] and $Na_2(NH_4)_8[H_2W_{12}O_{42}]\cdot 12H_2O$.[36] The $[H_2W_{12}O_{42}]^{10-}$ anion consists of two $HW_3O_{13}$ groups and two $W_3O_{14}$ groups that are connected by corner sharing. The two $HW_3O_{13}$ groups contain three edge-sharing $WO_6$ octahedra (yellow polyhedra in Figure 2) and the two $W_3O_{14}$ groups contain two edge-sharing $WO_6$ octahedra (blue polyhedra in Figure 2). These are formed into a cluster having a central cavity containing two protons. A bond between one of the protons and O5 was confirmed using bond valence sum calculations on the O atom (Supporting Information, Figure S3, Tables S1 and S2). Each W atom in the $W_3O_{14}$ group has two terminal oxygens ($O_a$), whereas each W in the $HW_3O_{13}$ group has one terminal oxygen atom. There are two types of bridging oxygen between two W atoms ($O_b$): $O_{b1}$ bridges two W atoms in the same $HW_3O_{13}$ and $W_3O_{14}$ groups, whereas $O_{b2}$ bridges two W in different $HW_3O_{13}$ and $W_3O_{14}$ groups by corner-sharing. The third oxygen group is the bridging oxygen connecting three W atoms ($O_c$). There are two types of $O_c$: $O_{c1}$ bridging three W atoms only in the $HW_3O_{13}$ group, whereas $O_{c2}$ bridges three W atoms between the $HW_3O_{13}$ and $W_3O_{14}$ groups (Figure S3). Selected bond lengths within the $[H_2W_{12}O_{42}]^{10-}$ anion are listed in the Supporting Information (Table S2). The oxidation state of W is +VI, as confirmed using bond valence sum calculations (Supporting Information, Table S3).

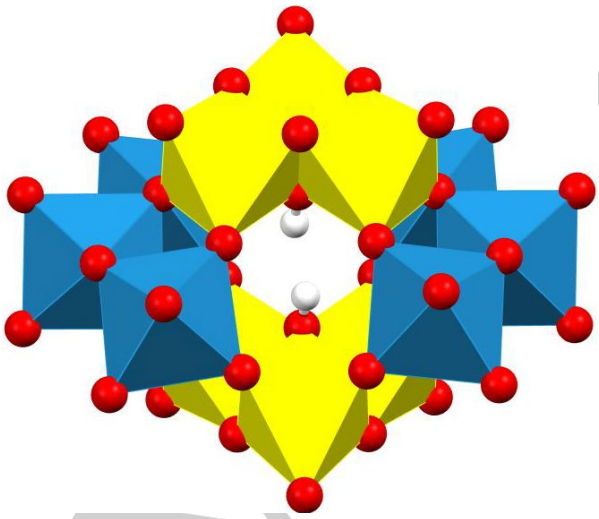

**Figure 2.** Polyhedral representation of the $[H_2W_{12}O_{42}]^{10-}$ anion. ($HW_3O_{13}$ groups, yellow polyhedra; $W_3O_{14}$ groups, blue polyhedra).

The powder XRD profiles of the wet solids (solids D (wet), F (wet), and E (wet)) are similar to the simulated powder XRD pattern obtained using the single-crystal X-ray data (Figure 3), indicating that the wet solids have the same crystal structure as that obtained by single-crystal structure analysis. The differences in peak intensities between the simulation and experimental results may be a result of the preferred orientation of the powder sample.

**Table 2.** Crystal data for $(CH_3NH_3)_{10}[H_2W_{12}O_{42}]\cdot 12H_2O$.

| Empirical formula | $C_{10}H_{86}N_{10}O_{54}W_{12}$ |
|---|---|
| Formula weight (g/mol) | 3416.9 |
| Temperature (K) | 100(2) |
| Crystal system | Triclinic |
| Space group | $P\bar{1}$ |
| *a* (Å) | 9.4933(6) |
| *b* (Å) | 13.0547(8) |
| *c* (Å) | 13.5615(5) |
| α (°) | 107.630(1) |
| β (°) | 90.464(1) |
| γ (°) | 93.406(1) |
| *V* (Å$^3$) | 1598.34(17) |
| Z | 2 |
| $D_{calcd.}$ (g/cm$^{-3}$) | 3.542 |
| $\mu$ (mm$^{-1}$) | 21.605 |
| Radiation | Mo Kα (λ =0.71073 Å) |
| *F*(000) | 1528 |
| Crystal size (mm$^3$) | 0.11 × 0.08 × 0.06 |
| 2Θ range | 3.152 to 55.79° |
| Index ranges | $-12 \le h \le 12$ |
| | $-17 \le k \le 17$ |
| | $-17 \le l \le 17$ |
| No. of reflection collected | 19091 |
| No. of unique reflections | 7496 ($R_{int}$ = 0.027) |
| Data/restraints/parameters | 7496/76/424 |
| G.O.F. | 1.052 |
| *R* indexes [$I > 2\sigma(I)$] | $R_1$ = 0.0205; $wR_2$ = 0.0425 |
| *R* indexes [all data] | $R_1$ = 0.0247; $wR_2$ = 0.0436 |
| $(\Delta/\sigma)_{max}$ | 0.003 |
| $(\Delta\rho)_{max/min}$ (e Å$^{-3}$) | 0.955/−1.831 |

### Characterization of dried solids

Next, the dried solids were characterized, and the Fourier transform infrared (FT-IR) spectra of the wet and dried samples were found to be similar, suggesting that the structure of methylammonium paradodecatungstate is not changed by drying (Figure S3, b and c). The FT-IR spectrum of dried solid E (Figure 4, a) contains bands at 1269, 1416, and 1470 cm$^{-1}$, which can be attributed to $CH_3$-$NH_3^+$ rocking, $CH_3^+$ bending, and $NH_3^+$ bending, respectively. In addition, a band at 1505 cm$^{-1}$, which can be assigned to the deformation vibration of $NH_3^+$, was observed.[37,38] These bands are characteristic of the bonds in the methylammonium counter cation. The bands at 1596 and 3400 cm$^{-1}$ are attributed to O-H bond vibrations of ligated or lattice $H_2O$. By comparing IR of dimethylammonium paradodecatungstate reported by Kótai group,[39] the bands at 949 cm$^{-1}$ and 928 cm$^{-1}$ are assignable to the vibration of W=O and W(=O)$_2$, respectively, and those at 881, 852, and 817 cm$^{-1}$ are assignable to the

vibration of edge-sharing W-O-W. The bands below 1000 $cm^{-1}$ are similar to those reported for the paradodecatungstate anion in ammonium paradodecatungstate[40] and dimethylammonium paradodecatungstate,[39] but different from those of metatungstate ($[H_2W_{12}O_{40}]^{6-}$) and heptatungstate ($[W_7O_{24}]^{6-}$) (Figure 4).[41]

The presence of the paratungstate structure in the dried solids was also confirmed by Raman spectroscopy. Figure 5 shows the Raman spectrum of dried solid E, together with those of ammonium paradodecatungstate and methylamine hydrochloride. The Raman band around 950 $cm^{-1}$ is assigned to the symmetric stretching of W=O bonds, and those at 860 $cm^{-1}$ is assigned to the asymmetric stretching of W=O bonds.[42] The bands of a deformation mode of $W(=O)_2$ group are observed at 394, 355, and 344 $cm^{-1}$, whereas the bands at 694, 645, and 569 $cm^{-1}$ are assigned to the stretching W-O-W bonds.[39] The spectrum of methylammonium paradodecatungstate is similar to that of ammonium paradodecatungstate, and the observed differences are related to the methylammonium bands. The Raman bands that indicate the presence of methylammonium as a counter-cation of paradodecatungstate anion were observed at 1004, 1467, and 1578 $cm^{-1}$ assigned to C-N stretching, $CH_3$ asymmetric bending, and $NH_3$ asymmetric bending, respectively.

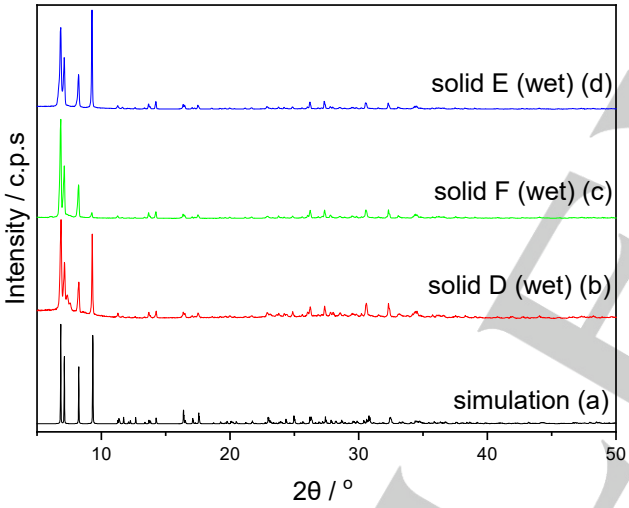


**Figure 3.** Simulated XRD patterns obtained using the single-crystal structure of $(CH_3NH_3)_{10}[H_2W_{12}O_{42}]\cdot 12H_2O$ (a), experimental XRD patterns of solids D (wet) (b), F (wet), and E (wet) (d).

The drying of the wet solids at 70 °C produced, without decomposition, another crystalline material containing $[H_2W_{12}O_{42}]^{10-}$. Crucially, the FT-IR spectra of the wet and dry samples are similar. Thus, the molecular structure of methylammonium paradodecatungstate was not affected by drying (Figure S3).

The XRD pattern of the dried solid was indexed, and the symmetry and cell dimensions were calculated using Fullprof. Figure S5 shows that the experimentally obtained pattern and simulated pattern of the dried solid match well. The space group was found to be triclinic $P\bar{1}$ ($a$ = 12.9207, $b$ = 12.2643, $c$ = 9.4324 Å, $\alpha$= 85.6309°, $\beta$= 102.6603°, $\gamma$ = 110.7095°). The unit cell volume (1364.11 $Å^3$) of the dried solid is smaller than that (1598.34 $Å^3$) of the wet solid, indicating that some crystal water molecules were lost on drying, thus reducing the unit cell volume. A similar change in the unit cell parameter with change in the number of lattice water molecules has been recently reported for dimethylammonium tungstate.[26] However, we could not obtain the detailed crystal structure using Rietveld analysis. In addition, the powder XRD pattern of the dried solid returned to that of wet solid by adding a small amount of water (Figure S4), indicating that the change in the crystal structure on the addition and release of water was reversible.

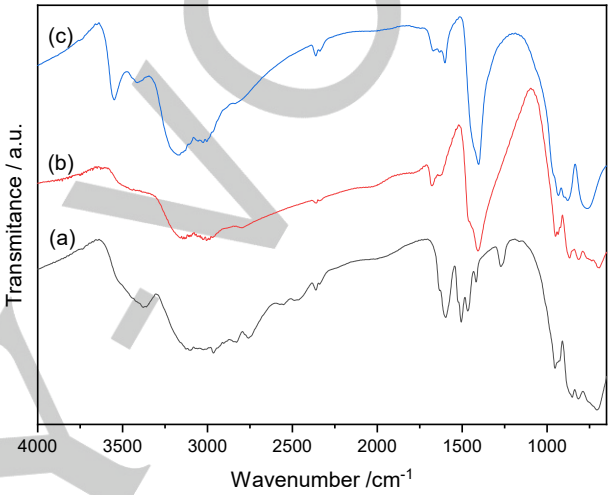


**Figure 4.** FT-IR spectra of solid E (methylammonium paradodecatungstate, $(CH_3NH_3)_{10}H_2W_{12}O_{42}$) after heating at 70 °C (a), ammonium paradodecatungstate ($(NH_4)_{10}H_2W_{12}O_{42}$) (b), and ammonium metatungstate ($(NH_4)_6H_2W_{12}O_{40}$) (c).

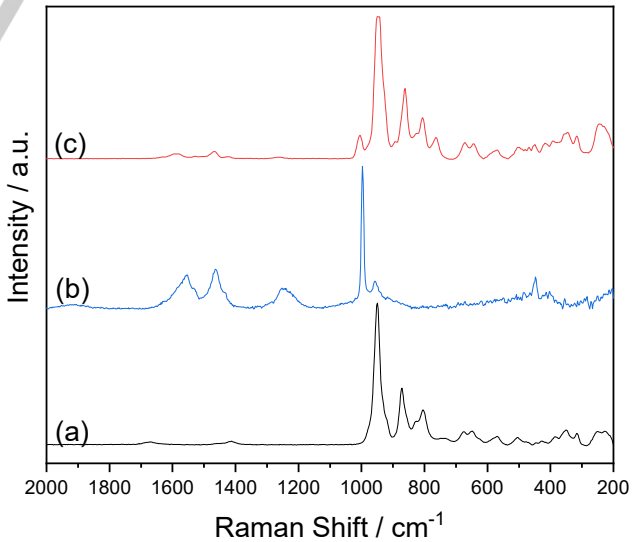


**Figure 5.** Raman spectra of ammonium paradodecatungstate, $(NH_4)_{10}H_2W_{12}O_{42}$ (a), methylamine hydrochloride, $CH_3NH_3^+Cl^-$ (b), and solid E (methylammonium paradodecatungstate), $(CH_3NH_3)_{10}H_2W_{12}O_{42}$ (c).

WILEY-VCH

In addition, the structure of $[H_2W_{12}O_{42}]^{10-}$ in water was confirmed by UV-Vis and $^{183}W$ NMR spectroscopy. The UV-Vis spectra of methylammonium paradodecatungstate, ammonium paradodeecatungstate, and ammonium metatungstate were measured between 190 and 1100 nm in aqueous solution (Figure S6). The obtained spectrum of methylammonium paradodecatungstate exhibits two characteristic absorptions for the ligand-to-metal charge transfer in the polyanions. A strong absorption at 194 nm was assigned to the $p_\pi$ ($O_d$) → $d_{\pi^*}$ (W) transitions. The hardly noticeable absorption around 250 nm is assigned to $p_\pi$ ($O_{b,c}$) → $d_{\pi^*}$ (W) charge transfer transition in the tricentric bonds of POMs.[43,44] These results are consistent with reported UV-vis measurements of ammonium paradodecatungstate.[43] The absorption at 257 nm corresponding to metatungstate, $[H_2W_{12}O_{40}]^{6-}$,[43] was only observed in ammonium metatungstate in addition to the band at 194 nm.

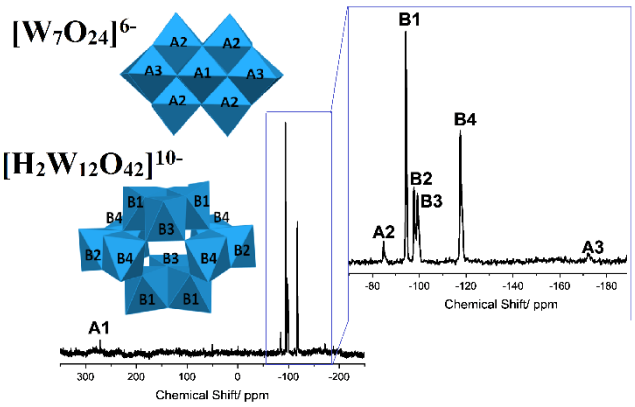


**Figure 6.** $^{183}W$ NMR spectrum of $(CH_3NH_3)_{10}[H_2W_{12}O_{42}]\cdot 3H_2O$ in $D_2O$.

Figure 6 shows the $^{183}W$ NMR spectrum of methylammonium paradodecatungstate in $D_2O$. The spectrum shows four singlets at -94.24, -97.73, -99.20, and -117.55 ppm with an estimated 2:1:1:2 integration ratio. These resonances correspond to the structure of the $[H_2W_{12}O_{42}]^{10-}$ anion.[46] In addition, three singlets at 271.32, -84.71, and -172.06 ppm having an intensity ratio of 1:4:2 were observed, corresponding to $[W_7O_{24}]^{6-}$. The presence of $[W_7O_{24}]^{6-}$ can be explained by (1) a small amount of $[W_7O_{24}]^{6-}$ being present in the solid and/or (2) the $[W_7O_{24}]^{6-}$ being in equilibrium between $[H_2W_{12}O_{42}]^{10-}$ and $[W_7O_{24}]^{6-}$ in aqueous solution.[47] It has been reported that $[W_7O_{24}]^{6-}$ is stable in solution, but $[H_2W_{12}O_{42}]^{10-}$ crystallizes from solution.[22] However, we do not know whether $[W_7O_{24}]^{6-}$ exists in the solid. Nevertheless, $[H_2W_{12}O_{42}]^{10-}$ is the main compound in both solid and aqueous solutions. These results indicate that the white solids produced by dissolving $WO_3$ and $H_2WO_4$ in aqueous methylamine solution and subsequent drying are both methylammonium paratungstate, $(CH_3NH_3)_{10}H_2W_{12}O_{42}$, which is stable after drying at 70 °C.

**Thermal transformation of $(CH_3NH_3)_{10}[H_2W_{12}O_{42}]\cdot 12H_2O$ in air**

The thermogravimetry (TG) and differential thermal analysis (DTA) curves of solid E (wet) in air flow (Figure 7) show four weight loss steps: the first (up to ca. 150 °C) and second (between ca. 190 and 250 °C) weight losses were accompanied by endothermic heat flow, whereas the third (around 300 °C) and fourth (around 460 °C) weight losses were accompanied by exothermic heat flow. The multi-step decompositions indicate that water and methylamine release in several steps from the compound. The results are in agreement with the TG-DTA of dimethylammonium dihydrogendodecatungstate hydrates that decomposition processes were found to be endothermic below 300 °C and exothermic above 300 °C.[48] The first weight loss can be ascribed to the release of $H_2O$. This weight loss (16.7%) corresponds to 36 mol of crystal water in 1 mol of methylammonium paradodecatungstate and it is higher than the number of lattice water molecules calculated from the single-crystal data. TG analysis detects not only water in the crystal but also water on the surface of the powder, which cannot be observed by single-crystal XRD measurements. Figure S7 shows the TG-DTA curves of the sample dried at 70 °C. In the first step, the 1.7% weight loss corresponds to three molecules of lattice water. The difference in these values may be due to the release of lattice water by drying at 70 °C. The effect of the loss of lattice water was discussed earlier (Figure S4).

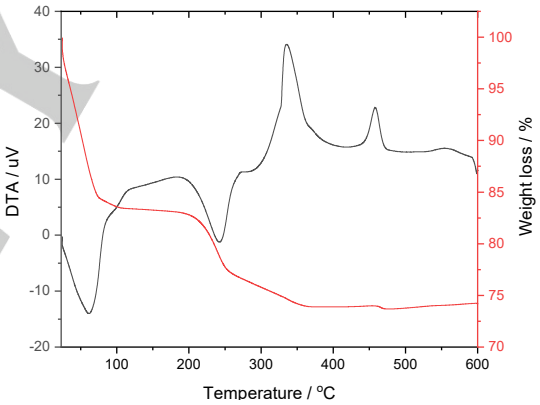


**Figure 7.** TG/DTA curves of solid E (wet) in air flow.

Figure 8 shows the TG/DTA and temperature programmed desorption-mass spectrometry (TPD-MS) curves of solid E, $(CH_3NH_3)_{10}[H_2W_{12}O_{42}]\cdot 3H_2O$, under helium flow. We observed several gasses with *m/z* of 44, 31, 30, 28, 18, 17, and 16. $CH_3NH_2$ shows *m/z* of 30, 31, and 28 with intensity ratio of 100/65/54; $H_2O$ shows *m/z* of 18, 17, and 16 with intensity ratio of 100/21/1; $NH_3$ shows *m/z* of 17 and 16 with intensity ratio of 100/80; $CO_2$ shows *m/z* of 44, 28, and 16 with intensity ratio of 100/10/10; CO shows *m/z* of 28 and 16 with intensity ratio of 100/3; $N_2O$ shows *m/z* of 44, 30, 28, and 16 with intensity ratio of 100/31/11/5; NO show *m/z* 30 and 16 with intensity ratio of 100/3; and $N_2$ shows *m/z* of 28. TPD-MS spectra showed that at temperature below 150 °C, only desorption of $H_2O$ was observed indicating that methylammonium as counter-cation was not desorbed at this temperature. By increasing temperature, beside the desorption of $H_2O$ (*m/z* = 18) and $CH_3NH_2$ (*m/z* =31), the degradation and

oxidized products such as $NH_3$, CO, $CO_2$, $N_2$, NO, $NO_2$, and/or $N_2O$ may be also observed. The formation of the degradation and oxidized products indicates a redox reaction between methylammonium and W=O has occurred. Similar degradation and oxidation of dimethylamine in dimethylammonium dihydrogendodecatungstate hydrates has been reported by Kótai group.[48]

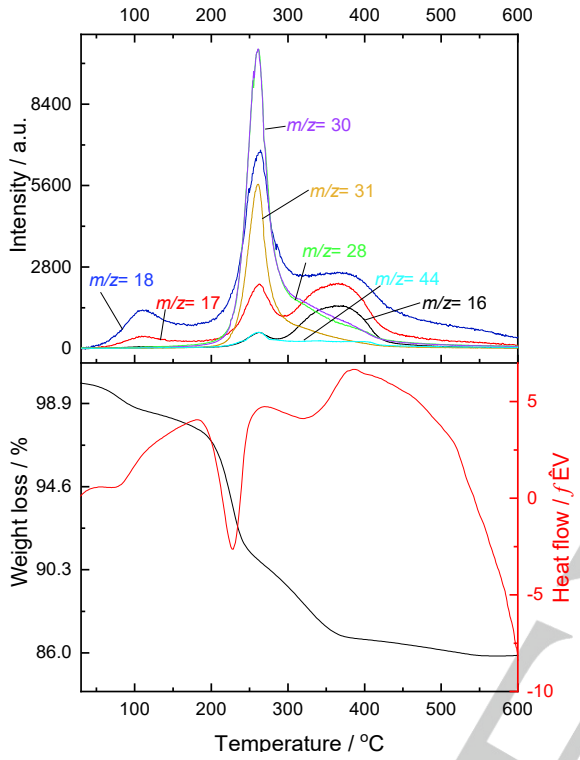


**Figure 8.** TG/DTA curves (bottom) and TPD-MS profile (top) of solid E ($(CH_3NH_3)_{10}[H_2W_{12}O_{42}]\cdot 3H_2O$).

Figure 9 shows the FTIR analysis results for the heated methylammonium paradodecatungstate. The intensity of the FTIR bands of $H_2O$ and $CH_3NH_2$ started to decrease when the temperature was higher than 200 °C, indicating that water and methylammonium were released on increasing the heating temperature and were completely removed at 400 °C. These results are consistent with the TG-MS analysis. The FTIR results also suggest that the $H_2W_{12}O_{42}$ structure is stable at temperatures up to 150 °C.

Figure 10 shows the XRD patterns of the heated methylammonium paradodecatungstate. The main peaks corresponding to methylammonium paradodecatungstate disappeared after heating the sample above 200 °C, and the release of water and methylamine from the sample caused the formation of an amorphous tungsten oxide. The amorphous $WO_3$ was transformed into monoclinic $WO_3$ after further heating at 350 °C. There was no formation of hexagonal $WO_3$, as observed in the heat-driven transformation of ammonium paradodecatungstate at approximately 400 °C.[40,49] The thermal transformation of methylammonium paradodecatungstate by heat treatment is shown in Scheme 3.

These results indicate that the methylammonium paratungstate $(CH_3NH_3)_{10}H_2W_{12}O_{42}$ is stable up to 150 °C, but further heating produces $WO_3$.

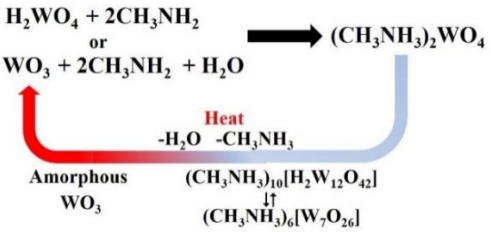


**Scheme 3.** Reaction of $WO_3$ and $H_2WO_4$ with methylamine and subsequent heating

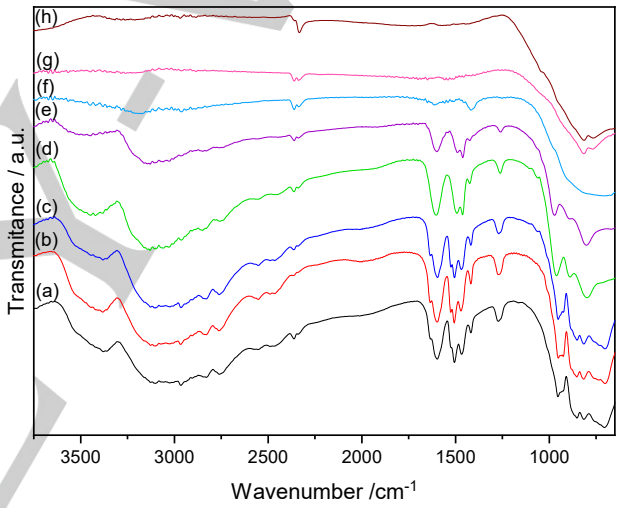


**Figure 9.** FTIR spectra of solid E (a) calcined at 100 (b), 150 (c), 200 (d), 250 (e), 300 (f), 350 (g), and 600 °C (h).

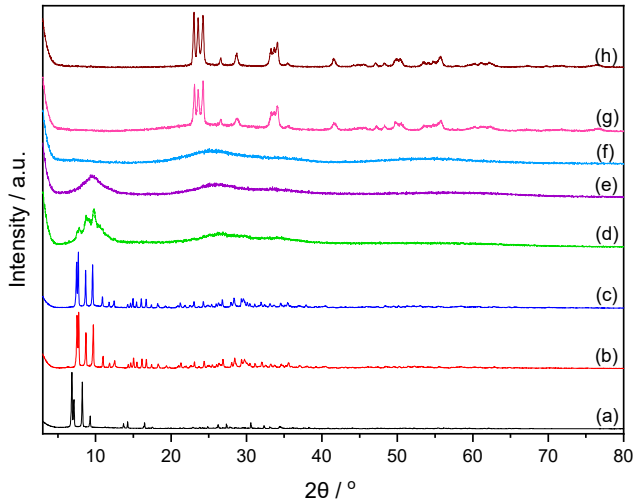

**Figure 10.** XRD patterns of solid E (wet) (a) heated at 100 (b), 150 (c), 200 (d), 250 (e), 300 (f), 350 (g), and 600 °C (h).

## Conclusions

We have described the synthesis, structural characterization, and heat-induced crystal transformation of methylammonium paradodecatungstate, $(CH_3NH_3)_{10}[H_2W_{12}O_{42}]\cdot 12H_2O$. Methylammonium paradodecatungstate was formed by the reaction of $WO_3$ or $H_2WO_4$ with methylamine and subsequent drying and was characterized in the solid state by single-crystal and powder XRD, FT-IR, and Raman spectroscopy and in solution by UV-Vis spectrometry and $^{183}$ W NMR measurements. A decrease in the unit cell volume was observed because of the release of crystal water on drying the solid at 70 °C, but the lattice water could be replaced by the application of a small amount of water. The methylammonium paradodecatungstate was stable up to 150 °C, and further heating produced an amorphous phase and then $WO_3$ by further heating in air. These results indicate that the white solid produced by Ekeley upon heating at 105 °C, one of the most used negative staining reagents, might not be methylammonium heptatungstate but, instead, methylammonium paradodecatungstate.

## Experimental Section

**Materials:** All chemicals were of reagent grade and were used without further purification. $WO_3$ and ethanol were purchased from Wako Pure Chemical Industries, Ltd., and 40% methylamine solution was purchased from Kanto Chemical Co., Inc. Ammonium metatungstate, ammonium paradodecatungstate, and $H_2WO_4$ were gifted from Nippon Inorganic Colour & Chemical Co., Ltd.

**Preparation of $(CH_3NH_3)_{10}H_2W_{12}O_{42}]\cdot 3H_2O$:** $WO_3$ (5.2 g, W: 22.5 mmol) or $H_2WO_4$ (5.63 g, W: 22.5 mmol) was mixed with 5 mL of 40% methylamine solution with a methylamine/W ratio of 2. The mixture was stirred for 30 min and introduced into a 50-mL Teflon-lined stainless-steel autoclave, which was heated at 70 °C for 2 h under static conditions in an electric oven. The resulting mixture was filtered to remove the white solid (3.1 and 1.0 g in the reactions of $WO_3$ and $H_2WO_4$, respectively). The solution was heated at 70 °C at atmospheric pressure to remove methylamine and water, and the solid (1.5 and 5.6 g in the reactions of $WO_3$ and $H_2WO_4$, respectively) were obtained. The amount of water was detected by TG analysis (weight loss = 3.19%, corresponding to 3 $H_2O$). Characteristic IR adsorption data, $\tilde{\nu}$/cm$^{-1}$(KBr): 3400(w), 1596(m), 1505(m), 1470(m), 1416(w), 1296(w), 949(s), 928 (s), 881(s, sh), 852(vs), 817(vs), 761 (s), 736(vs), 702(vs) cm$^{-1}$. Elemental analysis calcd. for $(CH_3NH_3)_{10}[H_2W_{12}O_{42}]\cdot 3H_2O$: H 2.11, C 3.69, N 4.30; found, H 0.86, C 3.97, N 4.22.

**Single crystals of $(CH_3NH_3)_{10}[H_2W_{12}O_{42}]\cdot 12H_2O$:** Single crystals of $(CH_3NH_3)_{10}[H_2W_{12}O_{42}]\cdot 3H_2O$ were formed by antisolvent vapor diffusion. The title compound was dissolved in water in a small bottle that was then placed in a larger bottle containing ethanol. After the large bottle was closed, ethanol slowly diffused into the small bottle. Colorless crystals suitable for single-crystal X-ray structure analysis were obtained after two days.

**Calcination of $(CH_3NH_3)_{10}[H_2W_{12}O_{42}]\cdot 3H_2O$:** $(CH_3NH_3)_{10}[H_2W_{12}O_{42}]\cdot 3H_2O$ was calcined in air at 100, 150, 200, 250, 300, 350, 400, 450, 500, 550, and 600 °C at a heating rate of 10 °C/min, and the temperature was maintained for 1 h.

**Analytical techniques:** Powder X-ray diffraction patterns were measured on a Bruker D2 PHASER 2$^{nd}$ Gen using Cu-$K_\alpha$ radiation. The samples were ground and placed on a sample holder, and the XRD profiles were recorded at $2\theta$ = 3–80°. FT-IR spectra were obtained using a NICOLET 6700 FT-IR spectrometer (Thermo Fischer Scientific) in the range of 650–4000 cm$^{-1}$ in KBr pellets. TG-DTA was carried out using a TG-DTA7300 instrument (SII, Japan) with air flow of 200 mL s$^{-1}$. Temperature programed desorption (TPD) was carried out using a BELCAT II – BELMASS system (MicrotracBEL Corp.) instrument under helium flow. The rate of temperature increase was 10 °C min$^{-1}$ and the maximum temperature was 600 °C. Ultraviolet–visible spectra were obtained using an Agilent 8453 UV-visible spectrometer in the range 190–1100 nm with a cell length of 1 cm. Raman spectra were collected using a Horiba Jovin Yvon T64000 with an $Ar^+$ 512-nm laser. The power of the laser was adjusted to 40 mW, and each spectrum was collected for 10 s and accumulated three times. and the maximum temperature was 600 °C. The $^{183}$W NMR spectrum was recorded on an ECA500 spectrometer (500 MHz, JEOL) at a resonance frequency of 20.839 MHz. The solution for $^{183}$W NMR was prepared by dissolving the sample in $D_2O$. The spectrum was referenced to an external 1 M $Na_2[WO_4]$ ($\delta$ = 0 ppm) standard. The powder XRD pattern of the dried solid was indexed using DICVOL06 in Fullprof. After performing Pawley refinement, the most reasonable space group was obtained.

**X-ray crystallography.** Single-crystal X-ray diffraction data of $(CH_3NH_3)_{10}[H_2W_{12}O_{42}]\cdot 12H_2O$ were collected at 100(2) K on a Bruker SMART APEX2 using Mo $K_\alpha$ radiation (Å = 0.71073 Å) monochromated by a layered confocal mirror. Data reduction and space group determination were carried out using the Bruker APEX 3 suite.[50] Absorption correction was applied using the multi-scan technique (SADABS).[50] The structure was solved by direct methods using SHELXT[51] and was refined using SHELXL[52] using the SHELXle[53] interface. The carbon and nitrogen atoms of the methylammonium cations were located in the electron density map, where the ammonium cations are hydrogen bonded to the anionic cluster. The hydrogen atoms of methylammonium cations were calculated using the riding model, whereas the hydrogen atom on O5 was located in the difference map. One lattice water molecule was disordered over two sites, and the hydrogen atoms were not located. All O–H distances were constrained to 0.84 Å, and the distance between H atoms in water molecules was fixed at 1.34 Å. All atoms, except hydrogen and a disordered water molecule, were refined anisotropically. CCDC 2082551 contains the supplementary crystallographic data of methylammonium paradodecatungstate, which can be obtained free of charge from the Cambridge Crystallographic Data Centre.

## Acknowledgements

This study was supported by JSPS KAKENHI, Grant Number JP19H00843 (Grant-in-Aid for Scientific Research (A)), JST A-STEP Grant Number JPMJTM20RF, International Network on Polyoxometalate Science at Hiroshima University, and JSPS Core-to-Core program. Mr. H. Fujitaka at the Natural Science Center for Basic Research and Development (N-BARD) at Hiroshima University is thanked for the $^{183}$W NMR measurements. We would like to thank Editage (www.editage.com) for English language editing.

**Keywords:** polyoxotungstate • methylammonium tungstate • thermal transformation

[1] M. T. Pope, Heteropoly and Isopoly Oxometalates, Springer–Verlag, Berlin, **1983**.
[2] C. L. Hill, *Chem. Rev.* **1998**, *98*, 1–2 (and articles within this special POM-themed issue).
[3] L. Cronin, A. Müller, *Chem. Soc. Rev.* **2012**, *41*, 7333–7334 (and articles within this special POM-themed issue).
[4] M. Sadakane, E. Steckhan, *Chem. Rev.* **1998**, *98*, 219–237.
[5] S. S. Wang, G. Y. Yang, *Chem. Rev.* **2015**, *115*, 4893–4962.
[6] I. A. Weinstock, R. E. Schreiber, R. Neumann, *Chem. Rev.* **2018**, *118*, 2680–2717.
[7] H. Lv, Y. V. Geletii, C. Zhao, J. W. Vickers, G. Zhu, Z. Luo, J. Song, T. Lian, D. G. Musaev, C. L. Hill, *Chem. Soc. Rev.* **2012**, *41*, 7572–7589.
[8] J. Zhang, Y. Huang, G. Li, Y. Wei, *Coord. Chem. Rev.* **2019**, *378*, 395–414.
[9] S. Ishikawa, Z. Zhang, W. Ueda, *ACS Catal.* **2018**, *8*, 2935–2943.
[10] H. N. Miras, L. Vilà-Nadal, L. Cronin, *Chem. Soc. Rev.* **2014**, *43*, 5679–5699.
[11] A. K. Jassal, R. K. Mudsainiyan, R. Shankar, *Mater. Chem. Front.* **2021**, *5*, 1090–1125.
[12] X. Li, X. Cao, W. Wang, Y. Yang, G. Rao, *Front. Chem. China* **2006**, *1*, 389–392.
[13] H. Yan, X. Zhang, S. Zhou, X. Xie, Y. Luo, Y. Yu, *J. Alloys Compd.* **2011**, *509*, L232–L235.
[14] M. Sadakane, K. Sasaki, H. Kunioku, B. Ohtani, R. Abe, W. Ueda, *J. Mater. Chem.* **2010**, *20*, 1811–1818.
[15] M. Tzaphlidou, J. A. Chapman, K. M. Meek, *Micron* **1982**, *13*, 119–131.
[16] B. D. Pandey, V. Kumar, D. Bagchi, R. K. Jana, Premchand, *Miner. Process. Extr. Metall. Rev.* **2001**, *22*, 101–120.
[17] Premchand, *Bull. Mater. Sci.* **1996**, *19*, 295–312.
[18] L. Fan, J. Cao, C. Hu, *RSC Adv.* **2015**, *5*, 83377–83382.
[19] H. N. Miras, J. Yan, D. L. Long, L. Cronin, *Angew. Chem., Int. Ed.* **2008**, *47*, 8420–8423.
[20] D. L. Long, P. Kögerler, A. D. C. Parenty, J. Fielden, L. Cronin, *Angew. Chem., Int. Ed.* **2006**, *45*, 4798–4803.
[21] D. L. Long, H. Abbas, P. Kögerler, L. Cronin, *J. Am. Chem. Soc.* **2004**, *126*, 13880–13881.
[22] N. I. Gumerova, A. Rompel, *Chem. Soc. Rev.* **2020**, *49*, 7568–7601.
[23] J. B. Ekeley, *J. Am. Chem. Soc.* **1909**, *31*, 664–666.
[24] J. W. van Put, *Int. J. Refract. Met. Hard Mater.* **1995**, *13*, 61–76.
[25] P. Zavalij, J. Guo, M. S. Whittingham, R. A. Jacobson, V. Pecharsky, C. K. Bucher, S. J. Hwu, *J. Solid State Chem.* **1996**, *123*, 83–92.
[26] G. Lendvay, E. Majzik, L. Bereczki, A. Domján, L. Trif, I. E. Sajó, F. P. Franguelli, A. Farkas, S. Klébert, P. Bombicz, C. Németh, I. M. Szilágyi, L. Kótai, *RSC Adv.* **2021**, *11*, 3713–3724.
[27] S. M. Morajkar, B. R. Srinivasan, *Indian J. Chem. A* **2021**, *60*, 185–195.
[28] C. A. Scarff, M. J. G. Fuller, R. F. Thompson, M. G. Iadaza, *J. Vis. Exp.* **2018**, *2018*, 1–8.
[29] A. Fera, J. E. Farrington, J. Zimmerberg, T. S. Reese, *Microsc. Microanal.* **2012**, *18*, 331–335.
[30] R. I. Glass, U. D. Parashar, *N. Engl. J. Med.* **2006**, *354*, 75–77.
[31] I. Istiqomah, Y. Kawato, M. M. Mahmoud, J. Okuda, M. Yasuike, Y. Nakamura, A. Fujiwara, K. Sahiro, M. Sadakane, T. Nakai, *Fish Pathol.* **2015**, *50*, 207–212.
[32] Y. Kawato, T. Mekata, T. Nishioka, I. Kiryu, T. Sakai, T. Maeda, S. Miwa, K. Koike, M. Sadakane, K. Mori, *Virology* **2021**, *559*, 120–130.
[33] M. J. G. Fait, H.-J. Lunk, M. Feist, M. Schneider, J. N. Dann, T. A. Frisk, *Thermochim. Acta* **2008**, *469*, 12–22.
[34] W. Han, M. Hibino, T. Kudo, *Bull. Chem. Soc. Jpn.* **1998**, *71*, 933–937.
[35] Z. H. Xu, X. L. Wang, Y. G. Li, E. B. Wang, C. Qin, Y. L. Si, *Inorg. Chem. Commun.* **2007**, *10*, 276–278.
[36] E. V. Peresypkina, A. V. Virovets, S. A. Adonin, P. A. Abramov, A. V. Rogachev, P. L. Sinkevich, V. S. Korenev, M. N. Sokolov, *J. Struct. Chem.* **2014**, *55*, 295–298.
[37] J. Padchasri, R. Yimnirun, *J. Alloys Compd.* **2017**, *720*, 63–69.
[38] S. Ishikawa, T. Murayama, S. Ohmura, M. Sadakane, W. Ueda, *Chem. Mater.* **2013**, *25*, 2211–2219.
[39] E. Majzik, F. P. Franguelli, G. Lendvay, L. Trif, C. Németh, A. Farkas, S. Klébert, L. Bereczki, I. M. Szilágyi, L. Kótai, *Z. Anorg. Allg. Chem.* **2021**, *647*, 593-598
[40] A. O. Kalpakli, A. Arabaci, C. Kahruman, I. Yusufoglu, *Int. J. Refract. Met. Hard Mater.* **2013**, *37*, 106–116.
[41] S. Ikenoue, M. Mikuriya, O. Miyauchi, R. Nukada, A. Yagasaki, *Bull. Chem. Soc. Jpn.* **1994**, *67*, 2590–2592.
[42] D. Hunyadi, I.M. Szilágyi, A.I. Tóth, E. Drotár, T. Igricz, G. Pokol, *Inorganica Chim. Acta* **2016**, *444*, 29-35
[43] S. Chaalia, J. C. Daran, A. Haddad, *J. Clust. Sci.* **2013**, *24*, 851–864.
[44] L. Wu, W. Yang, X. Dong, C. Yu, B. Liu, Y. Yan, H. Hu, G. Xue, *J. Coord. Chem.* **2015**, *68*, 2324–2333.
[45] L. R. Pizzio, C. V. Cáceres, M. N. Blanco, *Adsorpt. Sci. Technol.* **1992**, *9*, 36–47.
[46] J. J. Hastings, O. W. Howarth, *J. Chem. Soc., Dalt. Trans.* **1992**, *2*, 209–215.
[47] R. I. Maksimovskaya, K. G. Burtseva, *Polyhedron* **1985**, *4*, 1559–1562.
[48] L. Trif, F. P. Franguelli, G. Lendvay, E. Majzik, K. Béres, L. Bereczki, I. M. Szilágyi, R. P. Pawar, L. Kótai, *J. Therm. Anal. Calorim.* **2021**, *144*, 81-90
[49] J. Madarász, I. M. Szilágyi, F. Hange, G. Pokol, *J. Anal. Appl. Pyrolysis* **2004**, *72*, 197–201.
[50] Bruker, *APEX3, SADABS, SAINT*, **2016**.
[51] G. M. Sheldrick, *Acta Crystallogr., Sect. A: Found. Crystallogr.* **2008**, *64*, 112–22.
[52] G. M. Sheldrick, *Acta Crystallogr.*, *Sect. C Struct. Chem.* **2015**, *71*, 3–8.
[53] C. B. Hübschle, G. M. Sheldrick, B. Dittrich, *J. Appl. Crystallogr.* **2011**, *44*, 1281–1284

WILEY-VCH

**Entry for the Table of Contents**

Layout 1:

## FULL PAPER

Methylammonium paradodecatungstate was synthesized and characterized by single crystal and powder XRD measurements, FT-IR and Raman spectroscopy, and $^{183}W$ NMR analysis. Methylammonium paradodecatungstate is stable up to 150 °C, and transformed into amorphous and then monoclinic $WO_3$ by further heat treatment in air.

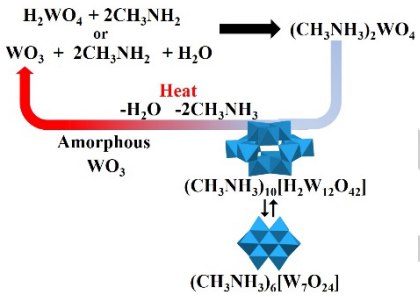


*N. C. Sukmana, Sugiarto, Z. Zhang, and M. Sadakane**

***Page No. – Page No.***

**Structure and Thermal Transformations of Methylammonium Tungstate**

WILEY-VCH

Additional Author information for the electronic version of the article.

Author: Ndaru Candra Sukmana ORCID identifier 0000-0003-3921-3655
Author: Sugiarto ORCID identifier 0000-0002-4190-2778
Author: Zhenxin Zhang ORCID identifier 0000-0002-9609-4691
Author: Masahiro Sadakane ORCID identifier 0000-0001-7308-563X

WILEY-VCH